Meteoritics & Planetary Science 39, Nr 7, 1169–1186 (2004)
Abstract available online at http://meteoritics.org

Composition of impact melt particles and the effects of post-impact alteration in suevitic rocks at the Yaxcopoil-1 drill core, Chicxulub crater, Mexico

Lutz HECHT,* Axel WITTMANN, Ralf-Thomas SCHMITT, and Dieter STÖFFLER

Institut für Mineralogie, Museum für Naturkunde, Humboldt-Universität zu Berlin, Invalidenstrasse 43, D-10115 Berlin, Germany
*Corresponding author. E-mail: lutz.hecht@museum.hu-berlin.de

(Received 22 September 2003; revision accepted 1 April 2004)

Abstract–Petrographical and chemical analysis of melt particles and alteration minerals of the about 100 m-thick suevitic sequence at the Chicxulub Yax-1 drill core was performed. The aim of this study is to determine the composition of the impact melt, the variation between different types of melt particles, and the effects of post-impact hydrothermal alteration. We demonstrate that the compositional variation between melt particles of the suevitic rocks is the result of both incomplete homogenization of the target lithologies during impact and subsequent post-impact hydrothermal alteration. Most melt particles are andesitic in composition. Clinopyroxene-rich melt particles possess lower SiO_2 and higher CaO contents. These are interpreted by mixing of melts from the silicate basement with overlying carbonate rocks. Multi-stage post-impact hydrothermal alteration involved significant mass transfer of most major elements and caused further compositional heterogeneity between melt particles. Following backwash of seawater into the crater, palagonitization of glassy melt particles likely caused depletion of SiO_2, Al_2O_3, CaO, Na_2O, and enrichment of K_2O and FeO_{tot} during an early alteration stage. Since glass is very susceptible to fluid-rock interaction, the state of primary crystallization of the melt particles had a significant influence on the intensity of the post-impact hydrothermal mass transfer and was more pronounced in glassy melt particles than in well-crystallized particles. In contrast to other occurrences of Chicxulub impactites, the Yax-1 suevitic rocks show strong potassium metasomatism with hydrothermal K-feldspar formation and whole rock K_20 enrichment, especially in the lower unit of the suevitic sequence. A late stage of hydrothermal alteration is characterized by precipitation of silica, analcime, and Na-bearing Mg-rich smectite, among other minerals. This indicates a general evolution from a silica-undersaturated fluid at relatively high potassium activities at an early stage toward a silica-oversaturated fluid at relatively high sodium activities at later stages in the course of fluid rock interaction.

INTRODUCTION

At the ICDP-Yaxcopoil-1 bore hole (Yax-1), a suevite-type, impact melt rock-bearing breccia sequence of about 100 m thickness was encountered (Dressler et al. 2003). This sequence allows an insight into the formation of the Chicxulub structure, which is one of the three largest and best preserved impact structures known on Earth. The impact structure has a diameter of about 200 km, was formed 65 Ma ago (Hildebrand et al. 1991; Dressler et al. 2003), and is located at the northern margin of the Yucatán peninsula in Mexico (Fig. 1). The Chicxulub impact event at the Cretaceous/Tertiary boundary is of general scientific interest, especially because of the association with a worldwide mass extinction (Alvarez et al. 1980; Hildebrand et al. 1991). The composition of proximal and distal ejecta deposits including the suevitic sequence at Yax-1 bear key information on the understanding of this mass extinction event (Smit 1999; Dressler et al. 2003). Impact melts deposited, for example, as coherent sheets, dikes, breccias (e.g., suevites), and spherules also provide important information on cratering processes on Earth and other planetary bodies in general (Grieve et al. 1977). Although melts of large impact structures are generally rather homogeneous (Grieve et al. 1977; Dressler and Reimold 2001), exceptions to this rule exist, and heterogeneities are probably even common at the microscopic scale (See et al. 1998). Compositional heterogeneities in impact melt rocks can be the result of: a) incomplete mixing and homogenization of melts from different target rocks; b) unmixing of immiscible melts; and c) post-impact modifications like hydrothermal alteration. The major goal of this study is to characterize the compositional variation of the

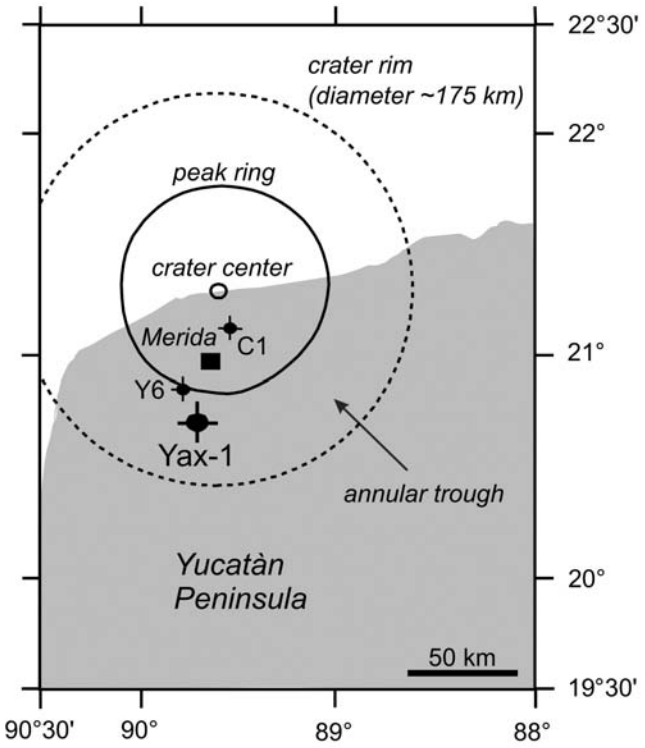

Fig. 1. Simplified geological map of the northern Yucatán peninsula. The Yax-1 drilling site is located ~60 km south of the center of the impact structure in the annular trough outside of the peak ring (based on Morgan et al. 1997, 2000, 2002). Selected PEMEX drilling sites (C-1, Y-6) are indicated.

impact melt particles from the suevitic sequence at Yax-1, with special emphasis on post-impact hydrothermal alteration, to better distinguish between the different processes responsible for impact melt heterogeneity.

SAMPLING AND ANALYTICAL METHODS

During the first ICDP sampling campaign on the Yax-1 drill core (May 2002), 24 samples of the impactites from depths between 794.63 to 894.94 m were taken for petrographic and whole rock chemical analysis (see Schmitt et al. 2004). Nine representative samples were selected (Fig. 2) for more detailed studies. One sample of the suevitic dike within the Cretaceous carbonate rocks from the depth of 916.65 m was studied for comparison. For details on the dike, the reader is referred to Wittmann et al. (2004). A scanning electron microscope JEOL-JSM 6300 was used for imaging and qualitative analyses of minerals using an RÖNTEC energy dispersive analytical system. Electron microprobe analyses were performed on a JEOL JXA 8800 operating at 15 kV and 15 nA. Analyses were calibrated using Smithsonian international mineral standards. The counting times were 20 sec on peak and 10 sec on background. The beam size was varied between 1, 3, 8, and 50 μm. Large beam sizes of 8 and 50 μm were applied on fragile hydrous phases (e.g., smectites). A separate calibration was prepared for bulk analyses of melt particles and smectites with a 50 μm beam size.

PETROGRAPHY OF IMPACTITES AND MELT PARTICLES

General Characteristics of the Impactites

The 100 m of impactites at Yax-1 represents a complex layered sequence of suevite-type polymict breccias ("suevitic sequence") with a variety of shocked target rock fragments and melt particles embedded in a clastic calcite-rich matrix (Fig. 2). This sequence was subdivided into 6 units based on variations in the nature, modal abundance, and grain size of clasts, melt particles, and matrix (Dressler et al. 2003; Stöffler et al. 2004).

The upper two units are greenish colored, melt-rich suevites with minor clastic matrix. The matrix consists of a very fine-grained mixture of calcite grains and silicate melt or rock fragments altered to clay minerals (smectites). The upper sorted suevite (unit 1) is fine-grained with a particle size generally less than 0.5 cm (sample Yax-1 800.25 m). In the uppermost part, it shows some laminations. The lower sorted suevite (unit 2) is less sorted and coarser grained with fragment sizes up to several cm (samples Yax-1 808.87 and 818.51 m, Fig. 2). The upper suevite (unit 3) is characterized by a seriate grain size distribution and abundant matrix. Typically, greenish to gray melt particles up to several cm in diameter display irregular twisted shapes and are embedded in a brownish-beige colored matrix (Fig. 2, sample Yax-1 824.01 m). The matrix is enriched in calcite compared to the upper and lower sorted suevite (units 1 and 2). The coarse-grained middle suevite (unit 4) is mostly brownish-beige in color, has a seriate grain size distribution, and consists of melt and carbonate fragments within a largely recrystallized matrix dominated by calcite (Fig. 2, samples Yax-1 848.38 and 852.80 m). The maximum sizes of clasts are 22 cm, 16 cm, and 4 cm for melt particles, crystalline rocks, and sedimentary rocks, respectively (Dressler, personal communication). Greenish colored melt particles within a light gray matrix also occur locally. Cavities filled with calcite that enclose barite were observed in sample Yax-1 852.80 m. The brecciated impact melt rock (unit 5) shows a variety of textures that, in part, can be called "monomict cataclastic melt rock" (Fig. 2, see sample Yax-1 865.01 m). This unit comprises the least-altered and well-crystallized cpx-rich melt particles that are embedded in a brownish matrix (sample Yax-1 865.01 m). Sample Yax-1 879.58 m is a green colored, coarse-grained, monomictly brecciated melt rock within a fine-grained, polymict, carbonate-rich matrix. The lower suevite (unit 6) is very coarse-grained (0.5 to 5 cm), polymict, and consists mainly of carbonate clasts, large silicate melt bodies, and a completely re-crystallized calcite-rich matrix (Fig. 2, Yax-1 894.26).

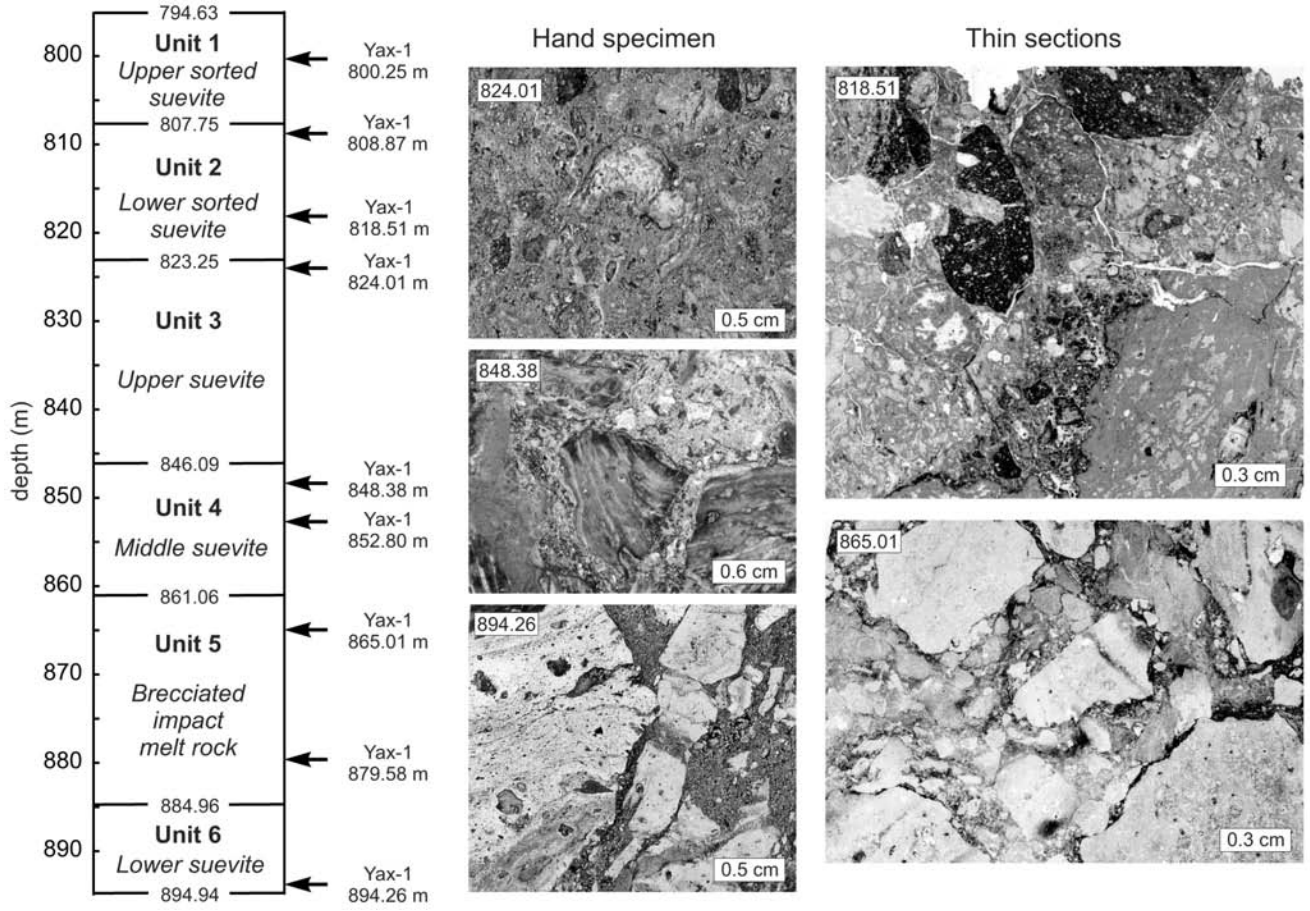

Fig. 2. Schematic profile of the impactite sequence at the Yax-1 drill hole showing the location of samples (see arrows) and some representative hand specimen and thin section images using parallel polarizing filters. The general subdivision of the suevitic sequence into 6 units is adapted from Dressler et al. (2003). The depth boundaries and names of the 6 suevite units are adapted from Stöffler et al. (2004).

Types of Melt Particles

At least four types of melt particles can be distinguished in the suevitic sequence based on particle shape, degree of primary crystallization, color, and chemical composition. Primary crystallization is defined as crystallization of minerals (e.g., plagioclase, clinopyroxene) from a melt or from a solid glass during early high-temperature stages after glass formation without any significant interaction with external fluids, e.g., before post-impact hydrothermal processes.

Type 1 melt particles are brownish to pale green and lack any primary crystallization, except remnants of devitrification spherulites (Figs. 3 and 4). The shape of these fragments is subrounded in most cases and rarely angular. Some large vesicles can occur (10 to several 100 μm), and particle margins may display porosity at the micrometer scale (Fig. 3b), both indicating degassing during cooling of the melt. Melt particles of type 1 have only been observed in samples from the upper three suevite units with a rough trend of decreasing frequency from top to bottom.

Type 2 melt particles are also pale green to brownish in color and may contain abundant vesicles, up to about 30 vol% (Fig. 3d). Smaller particles (<1 mm) of type 2 frequently exhibit angular shard-like shapes that probably formed due to broken-up vesicles (Fig. 5a). Some plagioclase microphenocrysts occur, in contrast to melt particles of type 1 (Fig. 3d). Rims of melt particle shards are frequently enriched in plagioclase microphenocrysts (Fig. 5a). Similar to type 1, the melt particles of type 2 were only observed in the upper three suevite units.

Type 3 melt particles are the most common in all suevite units, except in unit 1, where type 1 and 2 dominate. Type 3 melt particles are greenish to brown-beige colors and display sizes up to several cm. They comprise a variety of shapes in units 2 to 4, including uniform sub-rounded, elongated, lumpy, elongated, and twisted forms, and more angular forms in units 5 and 6 (Fig. 2). Type 3 melt particles are moderately to nearly completely crystallized with plagioclase and clinopyroxene laths, commonly displaying flow textures (Figs 4c, 5a, and 6a). An increase in the degree of crystallization with depth is evident from the samples of suevite units 2 to 4. Within

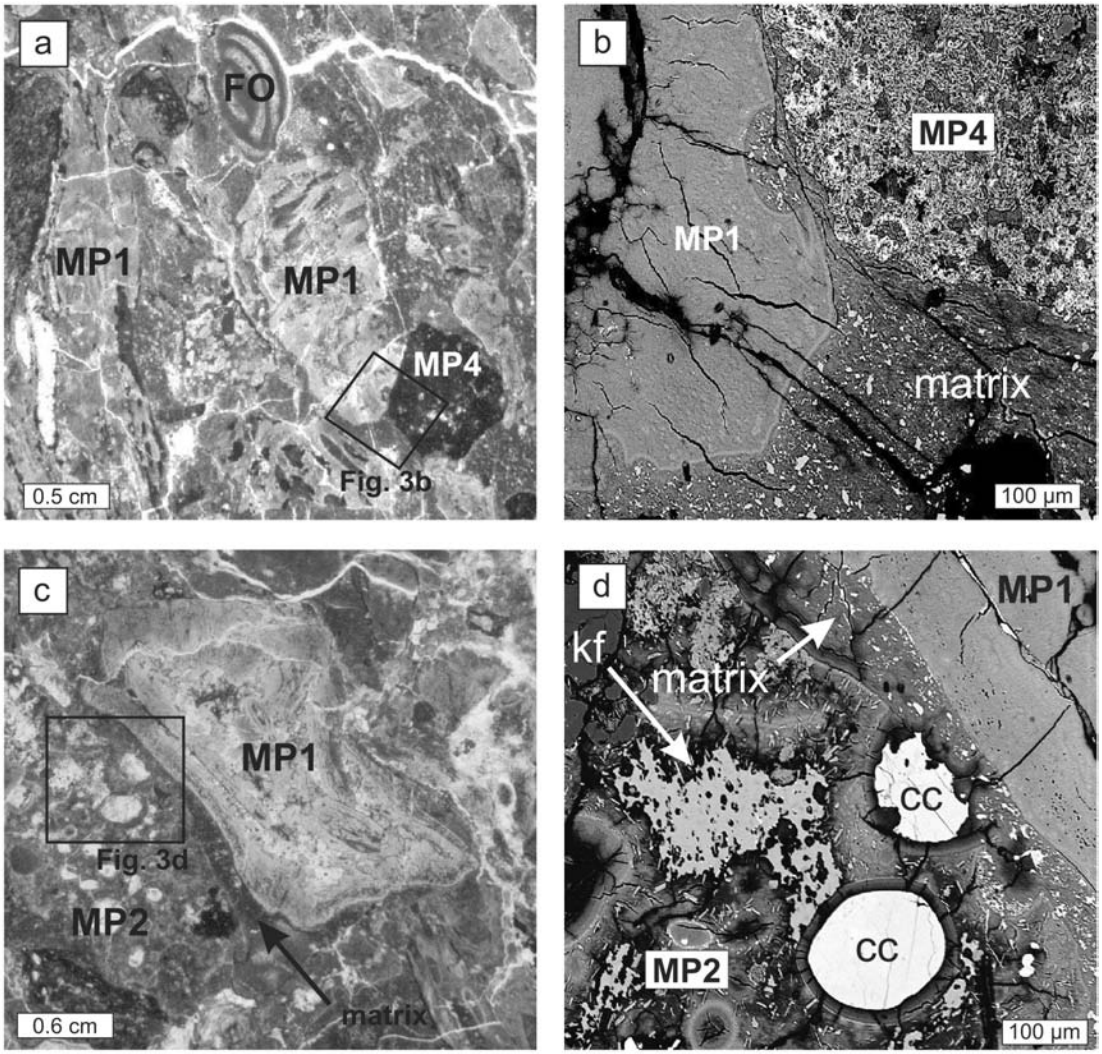

Fig. 3. Photomicrographs (a, c) using parallel polarizing filters and backscattered electron images (b, d) of sample Yax-1 800.25 m (unit 1): a) melt particles of type 1 (MP1) and 4 (MP4) and fossils (FO = foraminifera) embedded in a fine-grained clastic matrix; b) detail of (a) showing an altered glassy melt particle of type 1 in contact with a dark, aphanitic melt particle of type 4. Open vesicles at the margin of MP1 are filled by matrix material. The silicate matrix contains many small anhedral calcite grains (light gray spots); c) densely packed melt particles of type 1 and 2 and fossils with little matrix in between; d) detail of (c) at a contact between the clastic matrix and two melt particles. The type 1 melt particle (MP1) on the right shows a microporosity at the margin. The melt particle of type 2 (MP2) at the left has some plagioclase microphenocrysts and abundant vesicles, some of which are filled by calcite. Patchy replacement by secondary K-feldspar (kf) occurs in MP2.

units 4, 5, and 6, melt particles of type 3 are generally well crystallized (but aphanitic). Clinopyroxene is abundant in melt particles at the lowest two units of the suevitic sequence (Fig. 6). In units 2 to 4, microphenocrysts of clinopyroxene were only observed as inclusions within patches of secondary K-feldspar in type 3 melt particles (Fig. 4c).

Type 4 melt particles are dark brown to nearly opaque, subrounded to subangular in shape, and always display an aphanitic texture (Figs. 2, 3a, 3b, 4a, and 4b). They are generally rich in clasts of silicate or carbonate minerals (mostly quartz, feldspar, and calcite; see Fig. 4a). The melt particles of sample Yax-1 848.38 exhibit inhomogeneous texture locally with dark schlieren (see fragments of this sample in Fig. 2). They are believed to be transitional from type 3 to type 4 melt particles.

PETROGRAPHY AND MINERAL CHEMISTRY OF ALTERATION

Devitrification

Devitrification is probably one of the earliest processes of alteration that affected glassy melt particles in the suevitic sequence after quenching of melts. Spherulitic textures typical for devitrification processes are well-preserved in many vitric melt particles of type 1 and 2 in the upper suevite units

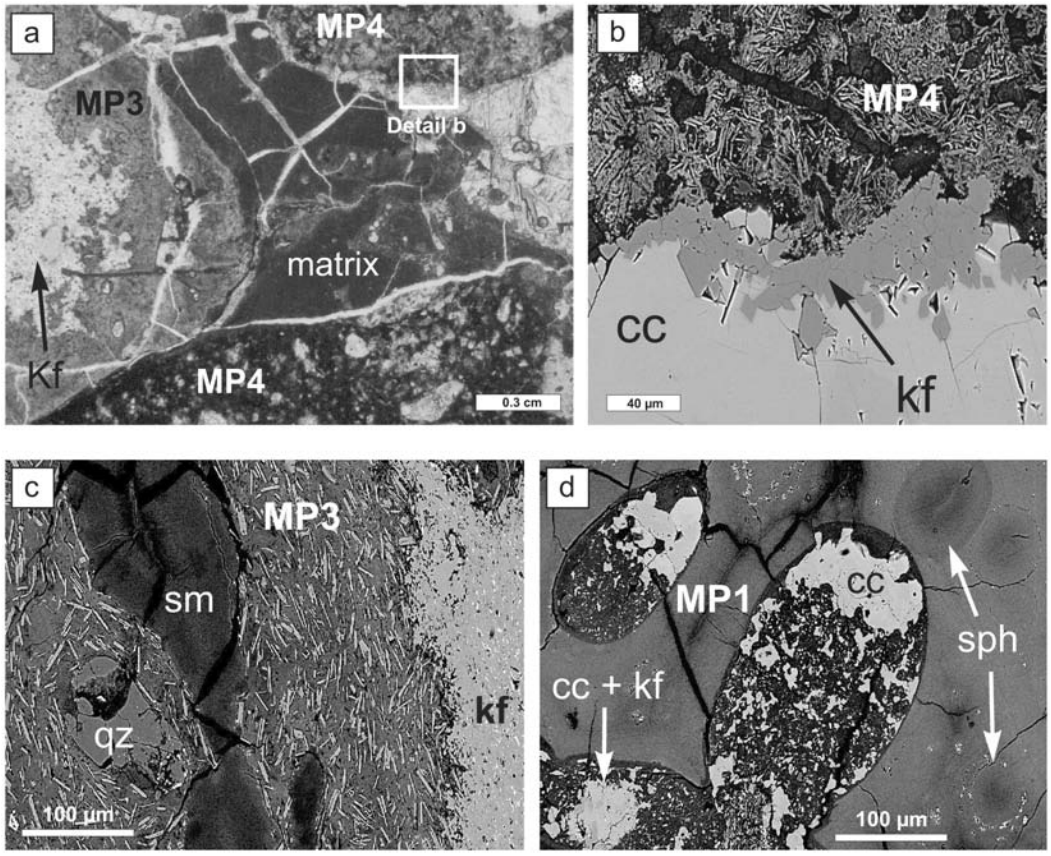

Fig. 4. Photomicrograph (a) using parallel polarizing filters and backscattered electron images (b to d) of sample Yax-1 818.51 m (unit 2): a) melt particles of type 3 (MP3) and 4 (MP4) and interstitial clastic matrix; b) detail of (a) showing void-filling K-feldspar (kf) and calcite (cc) at the margin of an aphanitic melt particle of type 4; c) detail of a type 3 melt particle with quartz inclusions, collapsed smectite-filled vesicles, and diffuse secondary K-feldspar (kf). Note the tiny clinopyroxene inclusions (bright spots) in the K-feldspar. The MP3 plagioclase microphenocrysts exhibit flow textures; d) detail of a melt particle of type 1 (MP1) with relic textures of spherulitic devitrification (sph). Vesicles are filled by a clastic matrix, which are locally overprinted by K-feldspar (kf) and calcite (cc).

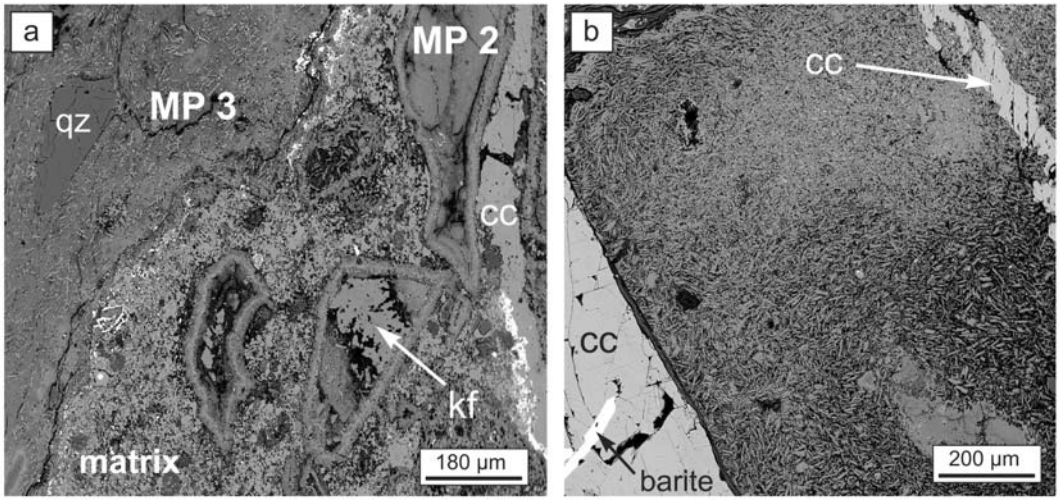

Fig. 5. Backscattered electron images of melt particles: a) melt particles of type 2 (MP2) and 3 (MP3) in a calcite-rich matrix in sample Yax-1 824.01 m. The MP2 particles exhibit a shard-like shape and plagioclase microphenocrysts at the margins. Secondary K-feldspar (kf) and calcite (cc) loclly occur in MP2 particles or in the matrix, respectively; b) plagioclase-rich melt particle in sample Yax-1 848.38 m, which is transitional from type 3 to type 4. See dark schlieren in melt particles in Fig. 2 (hand specimen) for comparison. The matrix is strongly replaced by secondary calcite (cc) with inclusions of barite. Calcite also occurs along fractures in the melt particle.

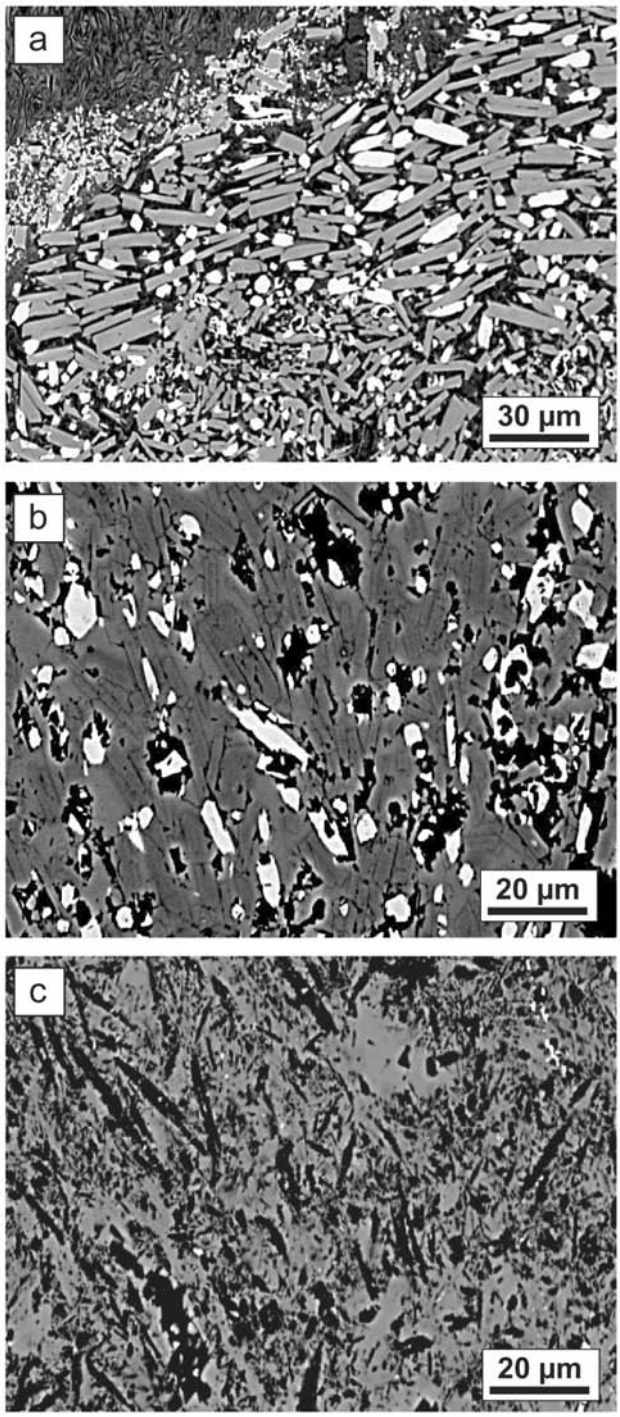

Fig. 6. Backscattered electron images of type 3 clinopyroxene-rich melt particles: a) almost unaltered clinopyroxene (white) and plagioclase (gray) -rich melt particle from sample Yax-1 865.01 m with some flow alignment at the particle margin. Late stage vein-filling smectite (sm3) is shown at the upper left corner; b) clinopyroxene (white) and plagioclase (gray) laths overgrown by secondary K-feldspar in a melt particle within sample Yax-1 879.58 m; c) melt particle in sample Yax-1 894.26 m with a similar texture as in (b) but clinopyroxenes are altered or dissolved (lath-shaped holes appear black). Replacement by secondary K-feldspar is pronounced.

(Fig. 4d), although they have all been pervasively altered to clay minerals (see below). Spherulites are frequently rimmed by tiny grains of Fe-Ti oxides (Fig. 4d). This suggests that the primary minerals forming the spherulites could not incorporate all Fe and Ti present in the glass.

Clay Minerals

Melt particles of type 1 and 2 and the glassy matrix of other types of melt particles were altered to a fine-grained mass of sheet silicates during palagonitization and subsequent hydrous alteration. There is some debate as to how palagonitization is defined, but most workers agree that palagonite is the transformation of (volcanic) glass to a fine-grained mass of smectites by interaction with a fluid phase (Stroncik and Schmincke 2002, and references therein). Here, the primary glass has been altered to smectites, called smectites of generation sm1 (Figs. 7a and 9). Iron and Ti oxides can be observed locally disseminated within the mass of smectites (Fig. 4d). Microprobe analyses of type 1 melt particles yield the bulk composition of smectite sm1, since the clays dominate the composition of these melt particles (Table 1). However, this has to be confirmed by a more detailed study using higher resolution techniques like the transmission electron microscope. The rims of vesicles in melt particles are generally decorated by fine-grained clay minerals, called smectite generation 2 (sm2; Fig. 7a). Smectite sm2 is variable in composition (Table 2) but differs from the bulk melt particle ("smectite 1") by lower K contents. Sheaves of smectites that grow inside of vecicles or along late fractures represent a third generation of smectite (sm3; Figs. 7). Fractures with smectite 3 crosscut zones of K-feldspar alteration, indicating that this smectite was formed at a late stage of post-impact hydrothermal alteration (Fig. 7b). Except for the alkalis, the chemical analyses of smectite 3 are rather homogeneous (Table 2). The composition is almost identical to analyses of Mg-rich saponites compiled by Newman (1987). Saponite is known as a typical void-filling smectite in altered basaltic glasses (e.g., Allen et al. 1982; Utzmann et al. 2002; Hagerty and Newsom 2003, and references therein).

The saponites (sm3) are K-poor and Na-rich compared to earlier formed smectites (sm 2; Table 2). This indicates an evolution from relatively high K activity fluids towards relatively high Na activity fluids from earlier to later stages of alteration. Saponite in veins is locally associated with calcite that formed in the center of saponite filled veins. In those cases, saponite (sm3) is also K-poor but is Ca-rich rather than Na-rich (e.g., Yax-1 852.80 m; Table 2), suggesting local equilibration with a Ca-rich fluid that also precipitated calcite.

K-Feldspar

Apart from palagonitization and smectite alteration, the formation of secondary K-feldspar is the most common

Table 1. Electron microprobe analyses of matrix and melt particles from the suevitic sequence in the Yax-1 drill core.[a]

Sample	Yax-1 800.25	Yax-1 808.87	Yax-1 818.51	Yax-1 824.01	Yax-1 800.25	Yax-1 800.25	Yax-1 808.87	Yax-1 818.51	Yax-1 800.25	Yax-1 824.01	Yax-1 800.25	Yax-1 808.87	Yax-1 818.51
Particle					P 07	P 01	P 07	P 02	P 02	P 08	P 05	P 02	P 06
Type	Matrix	Matrix	Matrix	Matrix	MP1	MP1	MP1	MP1	MP2	MP2	MP3	MP3	MP3
n	48	24	39	25	7	16	5	12	9	12	5	9	7
SiO_2 (wt%)	37.12	35.24	41.42	27.63	53.14	50.11	52.84	50.91	52.18	50.80	54.40	48.99	52.19
TiO_2	0.54	0.39	0.62	0.23	0.33	0.32	0.46	0.27	0.21	0.62	0.28	0.33	0.31
Al_2O_3	11.15	10.66	12.72	8.14	14.77	12.83	14.94	13.82	15.75	14.33	17.46	17.44	17.36
FeO	3.12	2.51	2.82	1.74	6.97	9.60	7.09	7.74	5.29	7.11	5.03	3.45	4.60
MgO	4.48	6.95	6.42	2.27	5.86	5.45	6.20	6.20	5.07	6.27	4.72	3.96	5.46
MnO	0.04	0.03	0.03	0.03	n.d.	0.02	0.01	0.02	0.01	0.01	0.02	n.d.	0.01
CaO	16.97	15.30	12.46	28.18	0.80	0.72	0.86	0.75	1.79	1.60	2.41	4.07	3.70
Na_2O	1.03	0.87	0.83	1.27	1.01	0.56	0.60	0.53	1.33	0.48	1.88	2.87	2.13
K_2O	1.27	1.03	1.40	2.92	3.26	4.98	3.80	4.25	2.53	4.32	2.09	1.85	2.64
Total	75.71	72.99	78.71	72.41	86.14	84.60	86.80	84.48	84.17	85.54	88.28	82.96	88.40
X_{Mg}	0.59	0.73	0.69	0.57	0.46	0.36	0.47	0.44	0.49	0.47	0.48	0.53	0.54
Sample	Yax-1 824.01	Yax-1 848.38	Yax-1 852.80	Yax-1 865.01	Yax-1 865.01	Yax-1 879.58	Yax-1 897.59	Yax-1 894.26	Yax-1 894.26	Yax-1 800.25	Yax-1 808.87	Yax-1 818.51	Yax-1 852.80
Particle	P 01	P 02	P 02	P 07	P 05	P 01	P 03	P 01	P 02	P 11	P 05	P 03	P 06
Type	MP3	MP3	MP3	MP3	MP3[b]	MP3	MP3[bc]	MP3[c]	MP3[c]	MP4	MP4	MP4	MP4
n	22	17	34	9	25	9	7	37	10	9	6	18	22
SiO_2 (wt%)	50.07	45.92	52.78	50.39	49.72	45.95	53.30	53.81	56.08	52.05	49.86	50.78	44.82
TiO_2	0.63	0.56	0.50	0.19	0.46	0.37	0.09	0.22	0.21	0.59	0.49	0.60	0.39
Al_2O_3	14.56	16.45	16.97	17.75	15.55	16.09	18.37	16.82	17.37	19.03	16.90	18.29	14.92
FeO	6.77	4.99	1.95	3.95	3.74	3.75	3.03	0.81	0.99	5.50	4.70	5.88	4.63
MgO	6.28	1.12	2.89	3.85	4.93	5.53	3.74	0.16	0.35	2.46	3.76	3.14	2.04
MnO	0.01	0.02	0.01	0.02	0.04	0.02	0.02	n.d.	0.01	0.02	n.d.	0.02	0.01
CaO	2.54	4.45	5.12	5.30	9.17	4.40	6.26	2.04	2.65	4.95	6.39	4.95	3.74
Na_2O	1.03	3.46	4.05	3.17	3.16	2.42	2.63	2.66	3.29	3.23	3.23	2.68	3.26
K_2O	3.92	3.47	3.92	3.08	1.93	1.98	4.29	8.35	7.51	1.83	2.22	1.97	2.36
Total	85.82	80.44	88.20	87.70	88.69	80.50	91.72	84.89	88.47	89.67	87.54	88.32	76.17
X_{Mg}	0.48	0.18	0.60	0.49	0.57	0.60	0.55	0.17	0.26	0.31	0.44	0.35	0.31

[a]Particle = number of melt particle; type = type of melt particle (see text for explanation); n = number of analyses; X_{Mg} = MgO/(MgO + FeO)
[b]Clinopyroxene-rich.
[c]Intensive K-metasomatism.

Table 2. Electron microprobe analyses of smectites from the suevitic sequence in the Yax-1 drill core.[a]

Sample	Yax-1 818.51	Yax-1 852.80	Yax-1 865.01	Yax-1 818.51	Yax-1 852.80	Yax-1 852.80	Yax-1 865.01
Generation	sm2	sm2	sm2	sm3	sm3	sm3	sm3
n	7	4	3	18	8	6	13
SiO_2 (wt%)	55.82	45.41	43.98	46.98	42.76	43.07	44.11
TiO_2	0.21	0.17	0.07	0.03	0.01	0.01	0.02
Al_2O_3	17.78	10.02	8.56	6.34	6.27	6.02	5.96
FeO	2.90	6.96	4.78	3.36	6.58	6.45	5.31
MgO	5.73	9.48	17.13	23.02	20.76	20.54	22.03
MnO	0.01	0.02	0.02	0.02	0.02	0.02	0.02
CaO	0.93	1.05	2.41	0.46	0.56	1.74	0.62
Na_2O	1.85	0.78	1.01	2.32	2.44	0.36	2.46
K_2O	1.83	2.69	0.88	0.11	0.20	0.07	0.09
Total	87.06	76.56	78.85	82.65	79.59	78.28	80.63
X_{Mg}	0.66	0.58	0.78	0.87	0.76	0.76	0.81

[a]Generation = generation of smectite (see text for explanation); n = number of analyses; X_{Mg} = MgO/(MgO + FeO)

alteration product of melt particles observed in all impactite units (Fig. 9). In most cases, irregular patches of anhedral K-feldspar are replacing parts of melt particles (Figs. 3d, 4a, 4c, and 6). This secondary K-feldspar preferentially nucleates in type 3 and 4 melt particles that already contain plagioclase microphenocrysts. Poikilitic textures occur when K-feldspar is replacing the melt matrix but not plagioclase or clinopyroxene microphenocrysts (Fig. 4c). Subhedral to euhedral K-feldspar is also a common void-filling mineral (Fig. 4b). The occurrence of secondary K-feldspar in melt rock dikes,

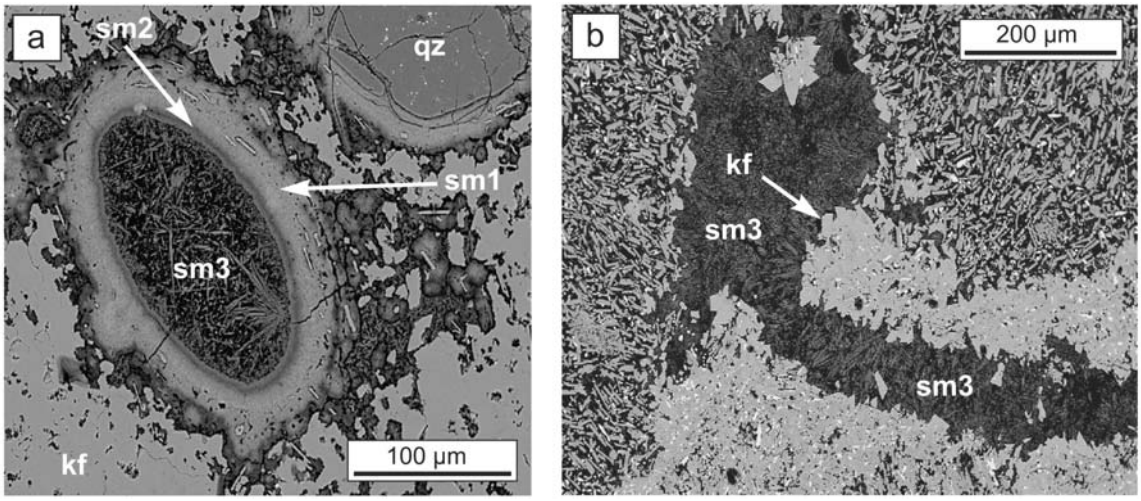

Fig. 7. Electron microscope images of different smectite generations: a) detail of a type 3 melt particle in sample Yax-1 818.51 m showing a vesicle filled by smectite generations 2 and 3. Smectite sm1 has replaced the plagioclase-bearing glassy matrix of the melt particle. Pervasive replacement of the melt particle by potassium feldspar (kf) is also shown; b) type 3 melt particles in sample Yax-1 865.01 m with a zone of potassium feldspar replacement (kf) cut by later vein-filling smectite (sm3).

suevitic dikes, and breccia dikes in the underlying Cretaceous sediments (see also Wittmann et al. 2004) indicates that the potassic alteration is not restricted to the suevitic sequence.

Alteration of Plagioclase and Clinopyroxene

Generally, plagioclase and clinopyroxene microphenocrysts are not altered. However, single fractured plagioclase phenocrysts in melt particles that are affected by K-metasomatism may exhibit potassium enrichment along fractures indicating alteration toward K-feldspar.

In moderately crystallized melt particles of type 3 (less than about 30 vol% plagioclase), microphenocrysts of clinopyroxene have only been observed in zones that are completely overgrown by secondary K-feldspar (Fig. 4c). This suggests that clinopyroxene microphenocrysts overgrown by early (?) K-feldspar can be preserved from later alteration stages. The absence of clinopyroxene elsewhere suggests that these later stages of alteration were able to dissolve or alter clinopyroxene but not plagioclase. This kind of protection of clinopyroxene was not always effective, as is demonstrated by the presence of melt particles from a strongly altered sample (894.26 m) of the lowest suevite unit 6 (Fig. 6). Although the melt particles with plagioclase and clinopyroxene were pervasively overgrown by secondary K-feldspar, the clinopyroxenes were selectively dissolved (Fig. 6c). Plagioclases were not affected by the late stage of alteration that followed early K-feldspar formation.

Calcite

Calcite is present in the suevitic rocks in many different textural relations. First of all, calcite occurs in calcite-bearing carbonate clasts or fossils and as a clastic component of the fine-grained suevite matrix. The presence of calcite that crystallized from carbonate melts was suggested by Dressler et al. (2003) and Stöffler et al. (2003, 2004). The amount of carbonate melt and the processes that have formed it, however, are still a matter of debate. Clear evidence exists for hydrothermal calcite precipitation in veins, voids, and vesicles within melt particles (Hecht et al. 2003; Lüders and Rickers 2004; Zürcher and Kring 2003). Voids and vesicles in the suevite sequence are commonly filled by drusy calcite. This calcite is contemporaneous with, or younger than, void-filling K-feldspar. They often occur together, but calcite always represents the final void-filling mineral (Fig. 4b). Two generations of drusy calcite exist. Under the optical microscope, early void-filling calcite is very rich in mineral and fluid inclusions, while later calcite is clear and almost free of any inclusions. With increasing depth, there is a general trend of increasing the degree of matrix replacement by secondary calcite (Fig. 5). In unit 4 and, especially, in unit 6, calcite is the dominant matrix mineral between the silicate melt particles.

Calcite is also a void-filling mineral in suevitic dikes and in the carbonate host rocks below the suevite unit (Hecht et al. 2003; Lüders and Rickers 2004). Primary dolomite is locally replaced by calcite in altered breccia dikes of the carbonate rock sequence below the impactites.

Quartz, Chalcedony, and Analcime

Corrosion of quartz grains by calcite was observed in zones of K-feldspar and calcite alteration. However, at a late stage, silica is reprecipitated, as shown by collomorphic void-filling quartz (chalcedony) that overgrows early K-feldspar and calcite in suevitic dikes (Fig. 8). The latest void-filling mineral is analcime (Figs. 8 and 9). In our preliminary study

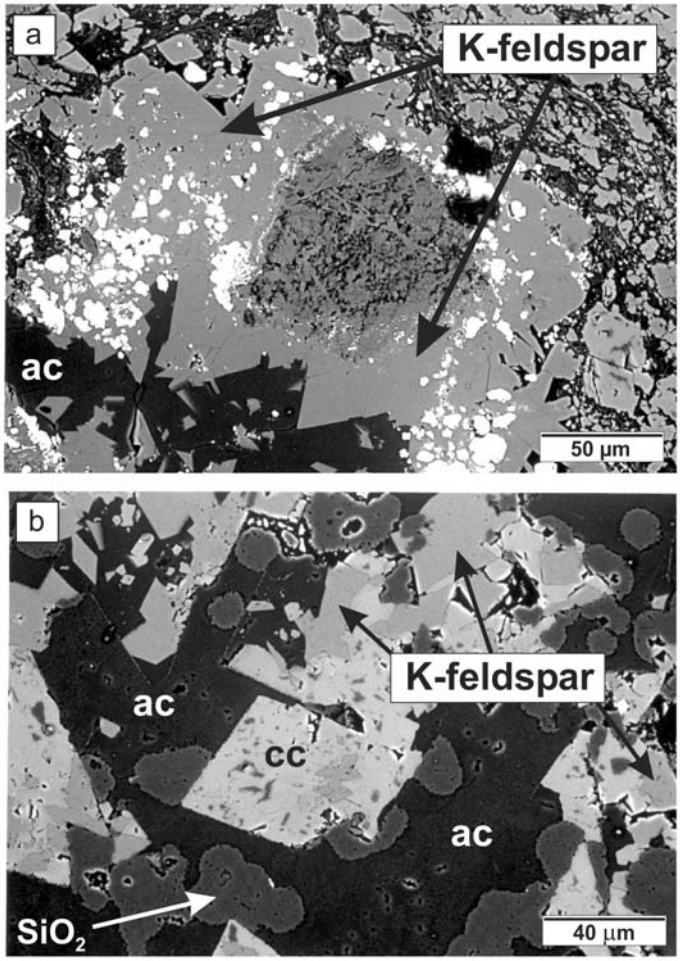

Fig. 8 Backscattered electron images of a suevitic dike (sample Yax-1 916.65 m): a) analcime (ac) is a late void-filling mineral following potassium feldspar that includes pyrite grains (white spots); b) colloform SiO_2 and analcime formed after K-feldspar and calcite (cc).

(Hecht et al. 2003), this pure Na-Al-silicate was assumed to be albite. Later, more detailed studies using electron microprobe and RAMAN analyses identified this mineral as analcime.

Other Minerals

Secondary calcite is locally associated with small grains of Sr-rich barite (Fig. 5b). Pyrite is rare in the lower part of the suevitic sequence but more abundant in the altered suevitic dikes and in altered parts of the sediments close to the dikes below the suevitic sequence. Intergrowths of pyrite and K-feldspar in suevitic dikes suggest that these minerals formed almost contemporaneously (Fig. 9).

COMPOSITION OF MELT PARTICLES AND SUEVITE MATRIX

The chemical composition of melt particles and suevite matrix was analyzed using an electron microprobe and a defocussed beam of 50 µm. Each analysis of a melt particle shown in the figures and tables represents a mean value of several microprobe analyses. A large number of analyses (up to 48) were carried out on the more heterogeneous melt particles or matrix. Representative mean values of suevite matrix and different types of melt particles from several samples are given in Table 1. Low totals of the microprobe analyses of melt particles are caused by the presence of hydrous minerals (e.g., clay minerals), calcite inclusions, and porosity due to minute vesicles or dissolved phases. Therefore, all melt particle analyses have been recalculated to 100% when discussed in the text or presented in binary plots to allow comparison with other chemical data from the literature. Since the recalculation procedure can be problematic, especially in case of mass transfer and volume changes due to hydrothermal alteration, element ratios or ternary plots are used for data presentation and discussion.

Melt particles

With some exceptions, most melt particles display SiO_2 contents between 57 and 63 wt%, which represents the

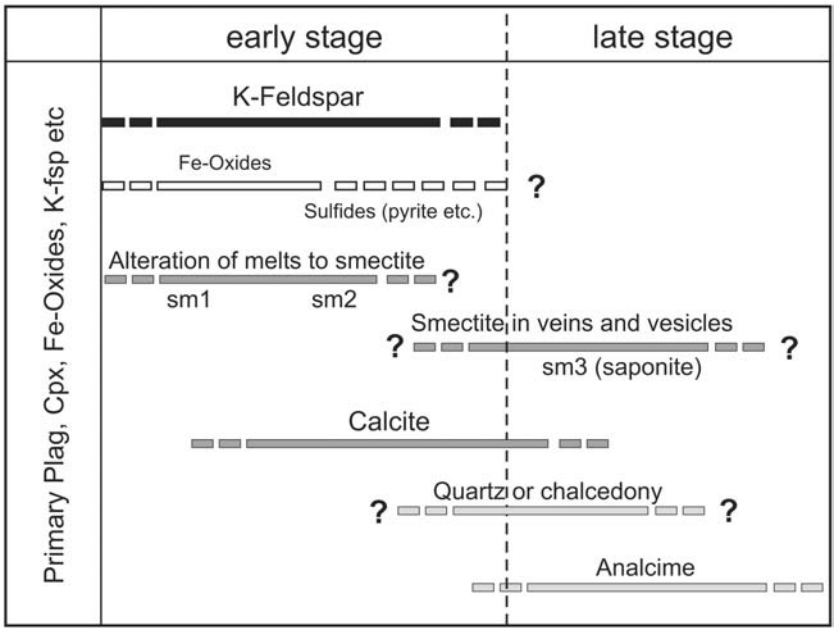

Fig. 9. Paragenetic sequence of the major alteration minerals in the impactites of the Yax-1 drill core.

typical range of andesites. Many of the other major element contents of the melt particles exhibit a wide range (e.g., Fig. 10). These include the alkalies that are very sensitive to hydrothermal alteration. Therefore, any rock classification based on these elements has to be performed with caution. For example, the extension of melt particle compositions from the andesite field toward the trachyandesite and trachyte field in Fig. 11 can be attributed to potassium enrichment during hydrothermal alteration (see discussion). Most melt particles exhibit relatively high Al_2O_3 and MgO contents compared to the continental crust and average impact melt rocks (Fig. 12).

The type 1 and 2 melt particles follow a similar compositional trend that is different from type 3 and 4 particles (Figs. 10 to 15). Type 1 and 2 are significantly depleted in CaO and Na_2O compared to the average continental crust and impact melts from Chicxulub and other large craters world-wide (Figs. 12 to 15). Furthermore, type 1 and 2 melt particles display a rather wide range in FeO und K_2O contents with a distinct trend of FeO and K_2O enrichment with SiO_2 and Al_2O_3 depletion (Fig. 12).

The melt particles of type 3 show the largest variation in chemical composition, which is related to the degree of primary crystallization (plagioclase and clinopyroxene) and the intensity of hydrothermal alteration. Particles in the upper suevite units, that only contain a few plagioclase microphenocrysts, have low CaO and Na_2O and elevated FeO and MgO contents similar to those of type 1 and 2 particles (Figs. 10 and 12). Particles with abundant clinopyroxene microphenocrysts have the highest CaO contents (Fig. 12). These melt particles are closest in composition to CaO-rich samples of the impact melt rocks derived from the Y-6 drill site (Figs. 10, 13, and 14) with the exception of MgO, which is much higher in melt particles from Yax-1 (Fig. 15).

On average, K_2O is enriched in melt particle type 3 compared to the continental crust and average impact melt rock (Figs. 10 and 14), although patches of secondary K-feldspar were not included in the microprobe analyses of melt particles, where they could be avoided. Melt particles of the lower suevite (unit 6) are pervasively altered by K-feldspar (Figs. 6b and 6c). In this case, secondary K-feldspar could not be avoided from the chemical analysis, which is evident from their high K_2O contents (Table 1, Fig. 12).

Most of the melt particles of type 3 have much higher MgO, and slightly lower FeO contents, than the average continental crust (X_{Mg} = 0.12) and reference impact melt (X_{Mg} = 0.28), which is especially evident from the high X_{Mg} (Table 1, Fig. 15).

Compositions of the dark aphanitic melt particles (type 4) are closest to the average continental crust and average impact melt rock (Figs. 10, 13, 14, and 15), although Al_2O_3 is enriched and SiO_2 is depleted in comparison (Fig. 12). Most particles of type 4 are andesitic and very similar in composition (Fig. 11). One particle has a higher SiO_2 content and resembles a dacite in composition (Fig. 11), although the FeO, MgO, and TiO_2 contents are rather high for a typical dacite (e.g., Fig. 13). Two particles plot in the trachyandesite field; however, some secondary potassium enrichment can not be excluded.

Suevite Matrix

The composition of the fine-grained clastic matrix was analyzed in the four suevite samples only from the upper three

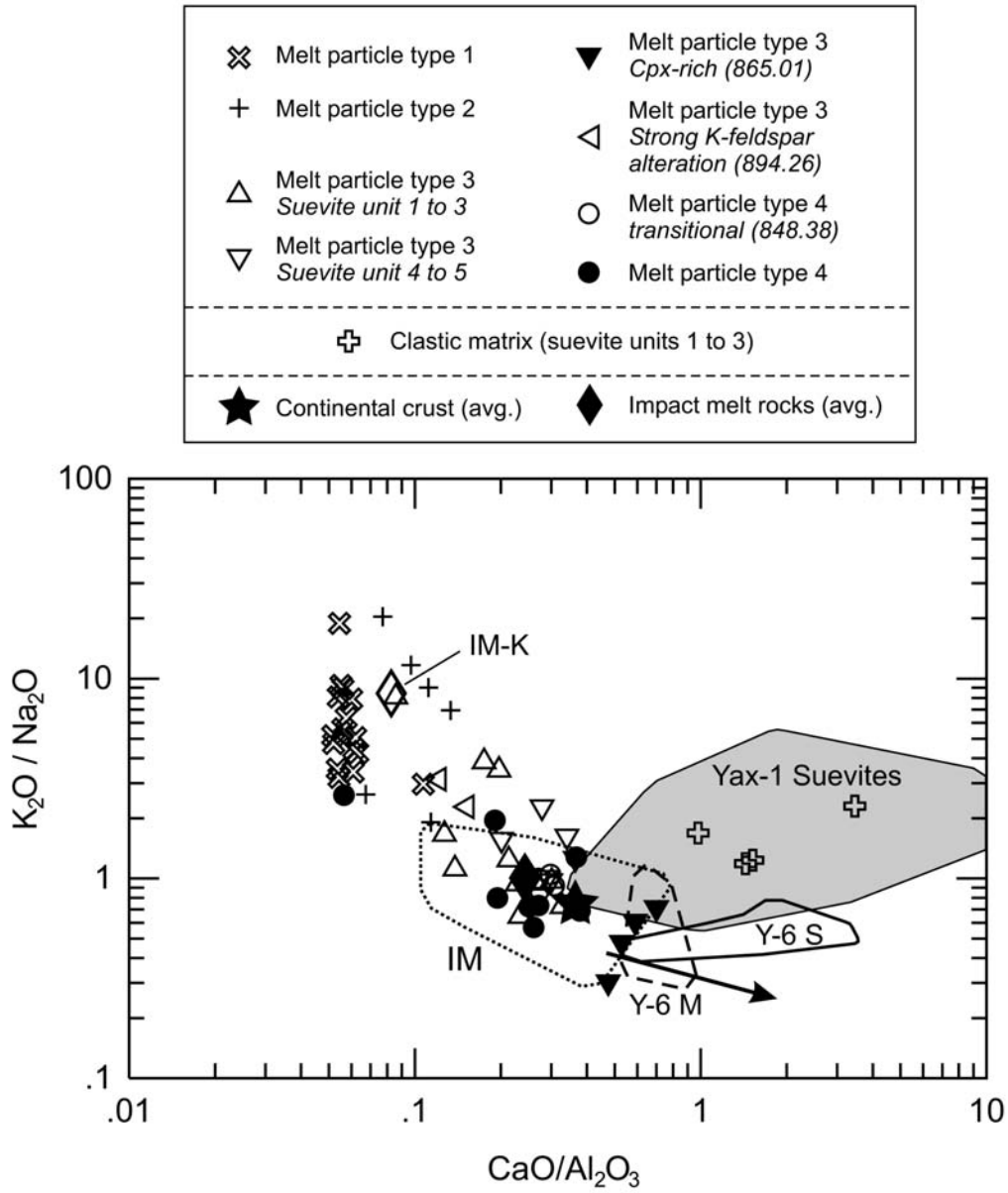

Fig. 10. CaO/Al_2O_3 versus K_2O/Na_2O plot of melt particles and clastic matrix from the Yax-1 suevitic sequence shown in comparison with Yax-1 S. Yax-1 S = whole rock composition of the suevitic sequence after Schmitt et al. (2004); Y-6 S = whole rock composition of suevites from the Y-6 drill core after Claeys et al. (2003); Y-6 M = impact melt rock composition at the Y-6 and C-1 drill core after Schuraytz et al. (1994) and Kettrup et al. (2000); IM = average values of impact melts of large (>3 km) impact craters world wide compiled by Dressler and Reimold (2001); IM-K = average composition of the impact melts of Ilyinets crater (Gurov et al. 1998), which is characterized by strong potassium alteration. The average of the continental crust is according to Wedepohl (1995), and the average of the impact melt rocks is according to Dressler and Reimold (2001). The arrow points from the average composition of the black glass toward the average composition of the yellow glass of the Haiti spherules (data from Koeberl and Sigurdson 1992).

suevitic units (Table 1). Below the suevitic unit 3, secondary calcite growth in the matrix is rather intensive, and chemical analyses would most probably not be representative of a primary clastic matrix. The suevite matrix in units 1 to 3 shows almost the same compositional trends as the whole rock samples of suevites from the Chicxulub crater (Figs. 10, 14, and 15). The composition of the suevites and its clastic matrix is largely determined by the mixing of two major target lithologies, the silicate basement rocks and the overlying mesozoic sediments, which are mainly Ca-dominated carbonate rocks and anhydrite. An increase in the Ca-rich sediment component is, therefore, characterized by a significant increase in CaO and related decrease in SiO_2, Al_2O_3, FeO, and other elements that are present in the silicate rock lithologies. This mixing trend was first proposed for the compositional variation of tektite-like glasses that originate

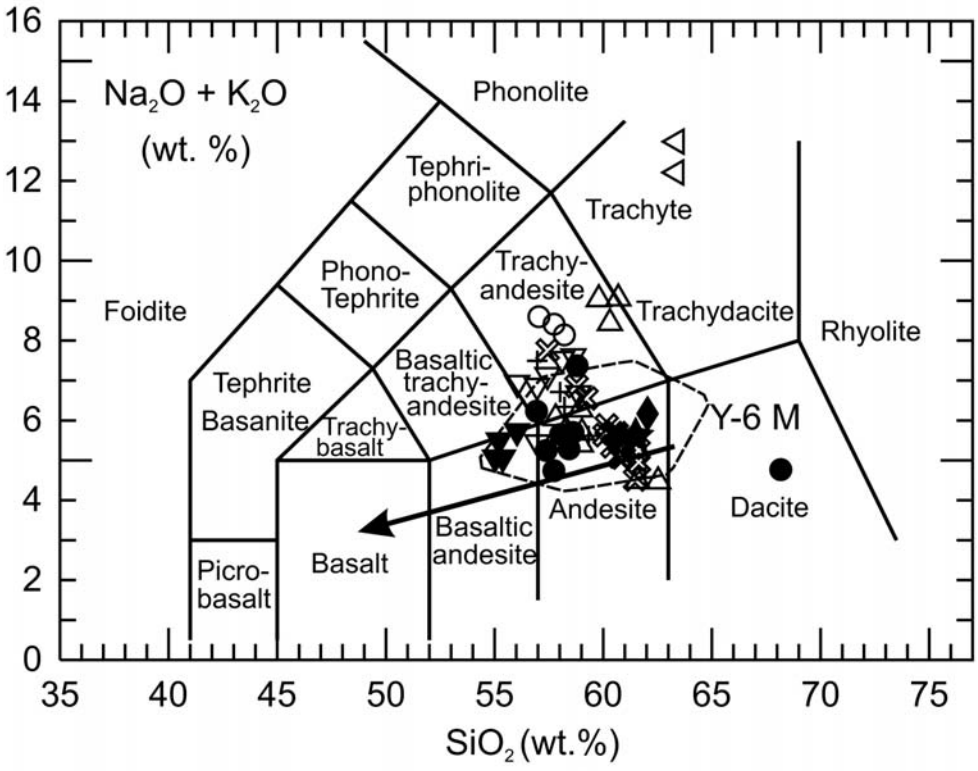

Fig. 11. SiO_2 versus $Na_2O + K_2O$ plot of melt particles from the Yax-1 suevitic sequence (rock classification after Le Bas et al. [1986]). The dashed line (Y-6 M) represents the impact melt rock composition at the Y-6 and C-1 drill core after Schuraytz et al. (1994) and Kettrup et al. (2000). For the symbol legend, see Fig. 10. Note that the microprobe analyses presented in this figure were renormalized to 100 wt%.

from the Chicxulub impact event (Sigurdsson et al. 1991) and is shown by an arrow in some figures for comparison.

The suevite matrix, as well as the whole rock samples of the Yax-1 suevites, have elevated K_2O/Na_2O ratios compared to the suevites from the Y-6 drill core (Fig. 10).

DISCUSSION AND CONCLUSIONS

Post-Impact Alteration Sequence

Post impact alteration is most probably induced by heat supplied to percolating fluids from the cooling impactites, as suggested for Chicxulub (Schuraytz et al. 1994) and many other impact structures (e.g., Allen et al. 1982; McCarville and Crossey 1996; Ames et al. 1998; Komor et al. 1988; Sturkell et al. 1998; Gonzales-Partida et al. 2000; Osinski et al. 2001; Hagerty and Newsom 2003). We would expect a paragenetic sequence from higher toward lower temperature alteration (e.g., McCarville and Crossey 1996), though their development and preservation strongly depends on the cooling history of the impact sequence. For example, early high temperature parageneses might not be developed due to fast cooling, or could be eliminated during longer lasting and more efficient stages of low temperature alteration.

A multi-stage post-impact hydrothermal alteration of the suevitic rocks at the Yax-1 drill site was recently proposed by Ames et al. (2003), Hecht et al. (2003), Lüders and Rickers (2004), and Zürcher and Kring (2003). The most detailed paragenetic sequence was presented by Zürcher and Kring (2003). They define three major stages: a) "Ca-Na-metasomatism;" b) "K metasomatism" involving K-feldspar, chlorite and calcite formation; and c) "burial or diagenesis" involving clay, calcite, and barite formation. The latter two stages are similar to our previous findings (Hecht et al. 2003). Zürcher and Kring (2003) also identified an early stage of high temperature Ca-Na-alteration, involving clinopyroxene (augite) alteration to hedenbergite and albite formation. However, until now, we did not find clear evidence for a high temperature Ca-Na-alteration that predates potassium alteration. We have not observed authigenic albite formation or albitization of plagioclase before K-feldspar formation as reported by Zürcher and Kring (2003). Furthermore, alteration of the vitric melt particles (type 1 and 2) has revealed significant depletion and not enrichment of CaO and Na_2O. If there was an early stage of high temperature Ca-Na-alteration, it was probably not very intensive. In addition, Ca- and/or Na-rich minerals from this stage could have been readily eliminated by later stages of hydrothermal alteration involving K-metasomatism and clay formation. It is difficult to establish a precise alteration sequence using a small number of samples. Based on petrographic observations and mineral chemistry, we only distinguish an early and late stage

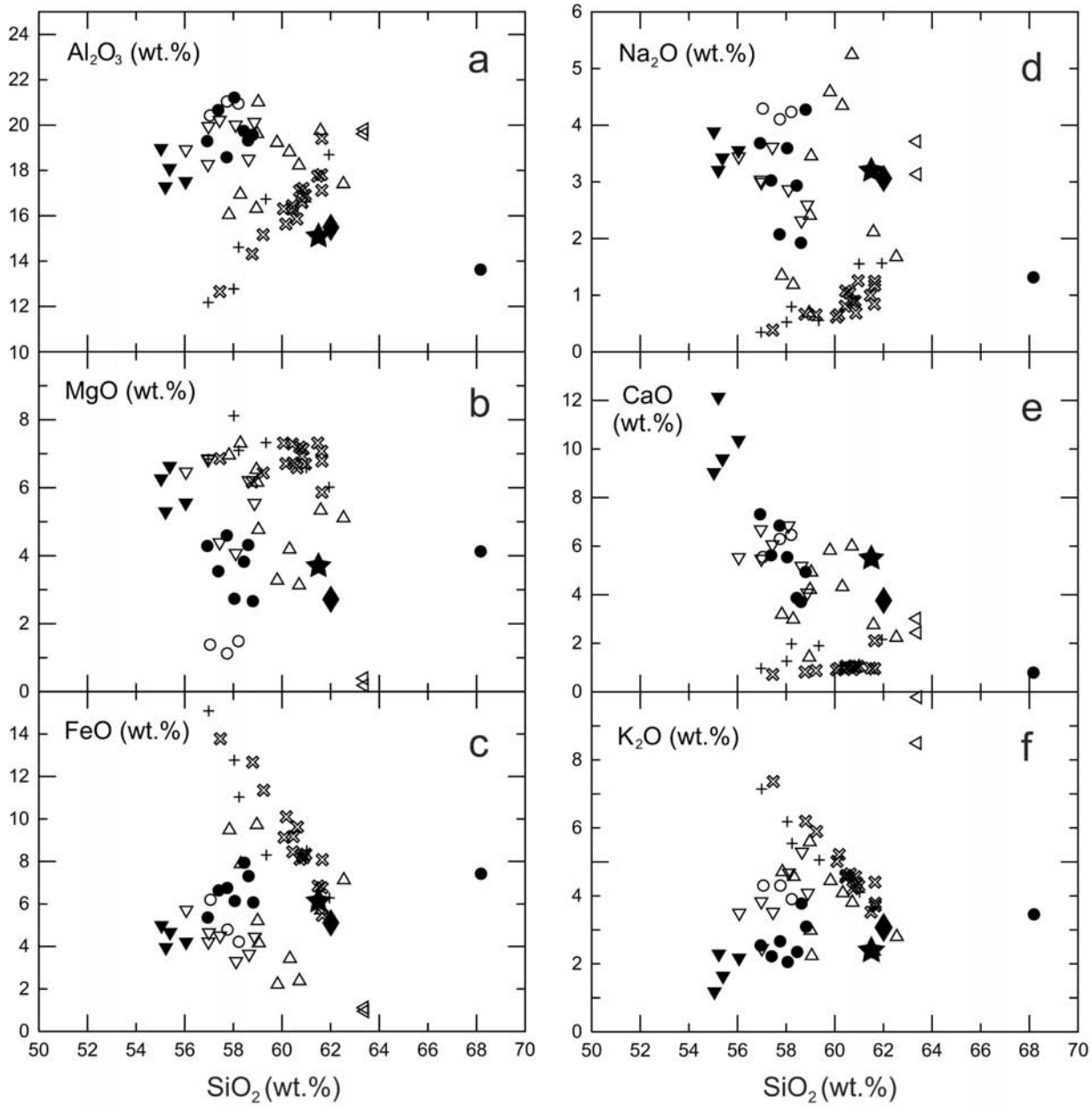

Fig. 12. Harker diagrams of melt particles from the Yax-1 suevitic sequence. The symbols are as in Fig. 10. The data are renormalized to 100 wt%.

of alteration (Fig. 9). Each of these stages may be further subdivided, but this needs a more detailed study based on more samples than were available for this study.

The early stage is mainly characterized by palagonitization of melt particles and the formation of secondary K-feldspar (K-metasomatism). During palagonitization, the glassy parts of the melt particles are transformed to clay minerals (smectites). During this stage, the SiO_2 content of glassy melt particles is depleted and clastic quartz grains become partly resorbed. These results suggest that the fluid was relatively rich in potassium and undersaturated in silica. Calcite crystallizes late during this early stage, either together or after the formation of K-feldspar. During the late stage, Na- and Mg-rich clay minerals (saponites) formed in voids and along veins that crosscut zones of K-feldspar alteration (Fig. 7b). In contrast to the early stage, silica precipitated during the late stage forming colloform aggregates (Fig. 8). Ames et al. (2003) also observed late low temperature colloform quartz in the suevite unit. Analcime represents the latest void-filling mineral in the altered suevitic dikes. The formation of quartz, Na-rich saponites, and analcime at the late stage indicates that the composition of the hydrothermal fluid developed from a low silica and high potassium activity at the early stage toward a

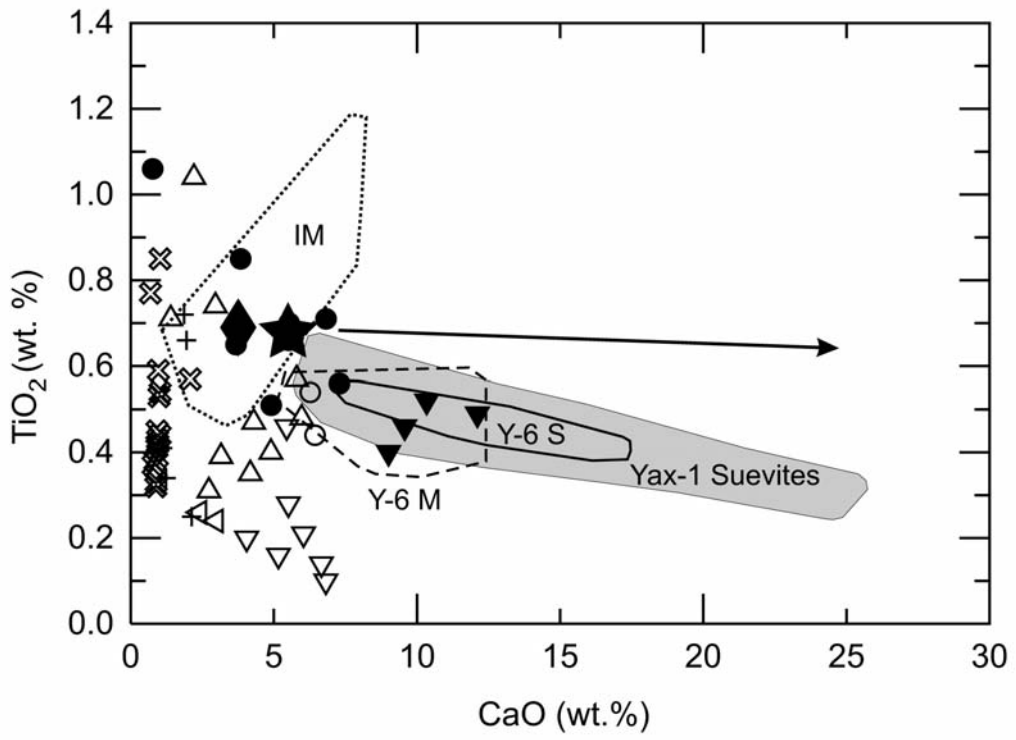

Fig. 13. CaO versus TiO_2 of melt particles from the Yax-1 suevitic sequence. The symbols and fields are as in Fig. 10. The data are renormalized to 100 wt%.

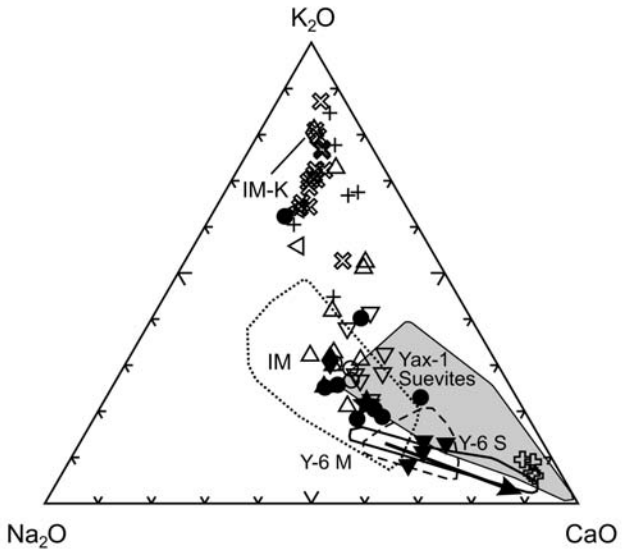

Fig. 14. Na_2O-K_2O-CaO plot of melt particles and clastic matrix from the Yax-1 suevitic sequence. The symbols and fields are as in Fig. 10.

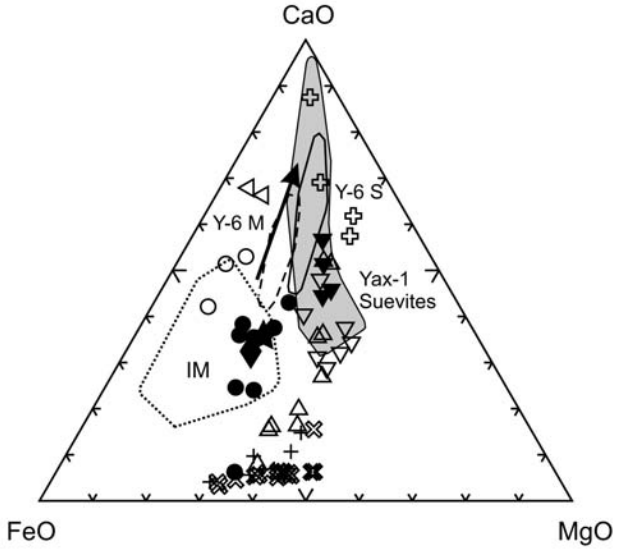

Fig. 15. FeO_{tot}-CaO-MgO plot of melt particles and clastic matrix from the Yax-1 suevitic sequence. The symbols and fields are as in Fig. 10.

higher silica and higher sodium activitiy at the late stage of alteration.

The very similar alteration paragenesis in the suevitic sequence and in the suevitic dikes below suggests that both lithological units were altered by the same hydrothermal fluids. This is especially evident from K-enrichment due to potassium metasomatism, which led to a general increase of the K_2O/Na_2O ratio (Figs. 10 and 16). This is further confirmed by fluid inclusion studies of late void-filling calcites that reveal the same fluid composition in both the suevite unit and the Cretaceous metasediments below (Lüders and Rickers 2004).

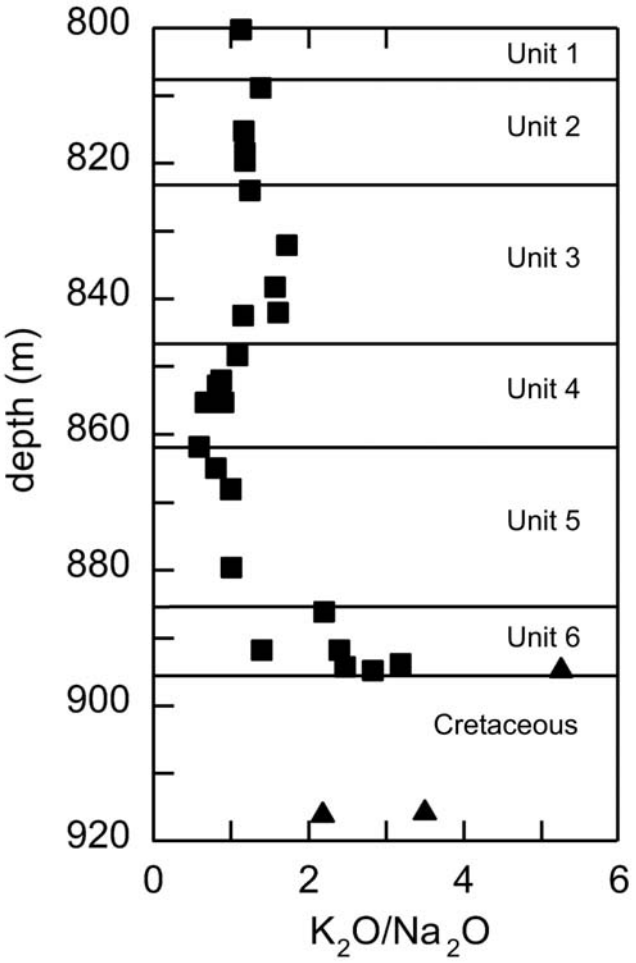

Fig. 16. K_2O/Na_2O of whole rock samples from the suevitic sequence (squares) and suevitic dikes (triangles) in the underlying Cretaceous sequence (data from Schmitt et al. 2004).

Hydrothermal Mass Transfer

Palagonite generally represents the first step of (volcanic) glass alteration and may involve depletion or enrichment of many elements, which depend on many parameters, such as temperature, the structure of primary material, fluid properties, etc. (Stroncik and Schmincke 2002, and references therein). Most studies on volcanic glass altered by seawater demonstrate that CaO, Na_2O, and SiO_2 are depleted and K_2O and FeO_{tot} are enriched during palagonitization (e.g., Peacock 1926; Moore 1966; Staudigel and Hart 1983; Berger et al. 1987; Zhou and Fyfe 1989; Alt 1995). In the case of FeO_{tot} it is often unclear, however, if iron is really enriched during palagonitization or if the increase of FeO_{tot}, results from passive accumulation due to volume loss. Some studies show that Al_2O_3 may also be depleted (Correns 1930), at least during early stages of palagonitization (Zhou and Fyfe 1989; Stroncik and Schmincke 2002). The same general compositional trend of palagonitization is shown by the melt particles of type 1 and 2 that are altered to smectite (sm1). The trend is characterized by K_2O and FeO enrichment with decreasing SiO_2, Al_2O_3, Na_2O, and highly depleted CaO contents (Fig 12). Volume changes during alteration can also change the content of a chemical component. If this is the case, the ratio between mobile (e.g., CaO) and immobile components (e.g., TiO_2) always remains constant. Since there are no constant ratios between TiO_2 and the other oxides, like CaO (Fig. 13), volume changes were not the prime factor for the alteration trend described above. Therefore, we suggest that the compositional variation of these melt particles (type 1 and 2) reflects a mass transfer, which is caused by interaction of the impact glass with seawater. It is very likely indeed that the glassy melt particles of the suevite unit quickly altered to palagonite during interaction with the seawater after return ("backwash") of the ocean into the crater.

The mass transfer associated with the alteration of the most abundant types of melt particles (type 3 and 4) depends on the degree of primary crystallization of these melt particles and the degree of subsequent hydrothermal alteration following palagonitization. A high degree of primary crystallization is generally associated with a high abundance of plagioclase microphenocrysts in relation to the glassy matrix of the melt particles. This accounts for their higher concentrations of CaO, Na_2O, and Al_2O_3 (Fig. 12). Alteration of the primary plagioclase of melt particles 3 and 4 was absent or very rare during both the palagonitization and subsequent hydrothermal alteration stages. Therefore, depletion of CaO, Na_2O, and Al_2O_3 in melt particles of type 3 and 4 during palagonitization was absent, or very limited, and was proportional to the amount of the primary, non-crystallized, glassy matrix present. The large amount of unaltered plagioclase in melt particles of type 3 and 4 is also the reason for higher Al_2O_3/SiO_2 compared to melt particles of type 1 and 2 because the latter have lost Al_2O_3 during palagonitization. The generally high MgO content of melt particles type 1 to 3 (Fig. 15) is most likely due to the formation of smectites with relatively high Mg/Fe ratios. In addition, the X_{Mg} of smectites increases from the early toward the late alteration stage (Table 2). High MgO content of the least-altered cpx-rich melt particles of type 3 (sample 865.01 m, Table 1) most probably do not result from alteration but, instead, reflect higher MgO contents of the melt (see Primary Composition of Impact Melts section below).

Although hydrothermal alteration of the Chicxulub impactites was recognized in drill cores Y-6 and C-1 (e.g., Schuarytz et al. 1994; Kettrup et al. 2000), it seems to be much more pervasive at the Yax-1 drill core. This is especially evident from intensive potassium metasomatism at Yax-1 (Hecht et al. 2003). Relatively high contents of K_2O and/or high K_2O/Na_2O ratios in melt particles, suevite matrix, and whole rock samples of the suevite unit at Yax-1 compared to Y-6 and C-1 (Figs. 10,12, 14, and 16) clearly demonstrate that potassium alteration was an important process in the suevitic

rocks at Yax-1. Potassic alteration of impactites within an impact-induced hydrothermal system has been demonstrated in many other cases (Grieve 1978; Reimold et al. 1994; McCarville and Crossey 1996; French et al. 1997) with a locally strong potassium enrichment (Gurov et al. 1998).

In the case of the Yax-1 suevitic rocks, a clear positive correlation exists between high whole rock K_2O contents and enhanced hydrothermal K-feldspar formation in voids and melt particles. This potassium enrichment is strongest in the deeper part of the suevitic sequence (unit 6) and in the suevitic dikes located in the underlying Cretaceous sediments (Fig. 16). An increase of potassium alteration toward lower sections of the altered impactite units has also been observed at other craters (Reimold et al. 1990; McCarville and Crossey 1996). This probably reflects the presence of ascending hydrothermal fluids, which precipitate most of the potassium already within the lowest section of the impactite unit.

Due to calcite precipitation, CaO is enriched in some of the strongly altered parts of the suevite unit; however, whole rock chemical analysis is not capable of distinguishing a hydrothermal addition of CaO since it cannot resolve the contribution of various amounts of carbonate rock fragments. In any case, petrographic observations indicate that hydrothermal calcite precipitation is locally important. Similar to potassium alteration, hydrothermal calcite formation is more pervasive toward the bottom of the suevite unit. Hydrothermal enrichment of Ba and Sr, as shown by anomalous whole rock values of sample Yax-1 852.80 m (Ba = 5900 ppm and Sr = 1420 ppm) compared to background values of the impactite unit (Ba = 215 ± 111 ppm and Sr = 396 ± 105 ppm; data from Schmitt et al. 2004), is demonstrated by the formation of Sr-rich barite associated with calcite in the matrix or in voids.

Primary Composition of Impact Melts

The determination of the primary impact melt composition is rather problematic in an environment in which significant post-impact hydrothermal alteration has occured. Since hydrothermal mass transfer was shown to be important in those melt particles that were least crystallized before the onset of post-impact alteration, we focus on the best crystallized melt particles of type 3 and on dark aphanitic melt particles (type 4), which show the least evidence of any alteration.

Most of the least-altered melt particles are andesitic in composition. One melt particle of type 4 possesses a higher dacitic SiO_2 content (Fig. 11), indicating that more acidic target lithologies may locally be involved and were not homogenized to the bulk andesitic impact melt. The compositional range of the impact melt particles is consistent with previous studies on Chicxulub impact melts at Y-6 and C-1 (e.g., Schuraytz et al. 1994). The melt particles of type 3 with a high modal amount of clinopyroxene and relatively high CaO and low SiO_2 contents, similar to those found at Y-6 (Figs. 12 and 13), might suggest the presence of mafic lithologies in the target rocks, e.g., basalts or basaltic andesites (Fig. 11). Contribution of a mafic precursor component was proposed for the Chicxulub impact melt by Kettrup et al. (2000) and for Chicxulub-related spherules by Schulte et al. (2003). However, petrological studies on the Ca-rich impact melt rocks at Y-6 demonstrate that a possible contribution of mafic rocks (diabases, pyroxenites, or amphibolites) must have been limited (Kring and Boynton 1992). We propose that the elevated CaO (and MgO) contents and reduced SiO_2 contents in the melt that characterize these clinopyroxene-rich particles result from the mixing of the silicate basement rocks with the overlying carbonate sequences. There are two main lines of evidence to support this: 1) the relatively low TiO_2 content of these melt particles is inconsistent with fusion of a mafic parental rock; and 2) the compositional analogy with Haiti glasses. If the clinopyroxene-rich melt particles had been formed by fusion of an average crustal rock (e.g., of andesitic composition) with a fusion component of mafic rock, like a high-Ca, low-Si basalt, we would expect higher TiO_2 contents. Only mixing with ultra mafic rocks would not increase the TiO_2 content but would not increase the CaO content either. An increase of CaO (and MgO) and decrease of SiO_2, without an increase of TiO_2, can result from mixing with carbonate rocks (with some dolomite involved). This mixing trend is exactly what we observe in Chicxulub suevites (Claeys et al. 2003; Schmitt et al. 2004) and Chicxulub related tektite-like glasses. Glassy material and spherules from Beloc (Haiti) are interpreted as tektite glasses that were ejected from Chicxulub (Sigurdsson et al. 1991; Kring and Boynton 1991). The chemical composition of the Haiti glasses suggest that they were formed by mixing between two bulk end member lithologies: a) upper continental crustal rocks of granitic or andesitic composition; and b) carbonate (and minor anhydrite) rocks (Sigurdsson et al. 1991; Bohor and Glass 1995). The abundance of carbonate rocks mixed with the silicate rocks is highest in the so called “yellow glass” that exhibits CaO contents up to 28 wt% (Bohor and Glass 1995). Such a high degree of mixing between the basement rocks and the more superficial carbonate rocks is only expected during the early stages of impact, when the process of jetting produces the well-mixed Ca-rich tektite melts (e.g., von Engelhardt et al. 1987). During later stages of excavation, the Chicxulub bolide mainly penetrated the crystalline silicate basement (Pierazzo and Melosh 1999), and impact melts formed at this time are expected to predominantly possess silicate rock compositions typical of average continental crust. Some mixing of silicate with carbonate material has occurred in the Chicxulub impact melts from Yax-1, although most probably less than in the Haiti glasses. Small variations in bulk composition of impact melt rocks at Y-6 and C-1 were also attributed to different proportions of assimilation of carbonate

sediments to silicate basement (Schuraytz et al. 1994). Therefore, we conclude that the chemical variation observed in the least-altered melt particles of Yax-1 is due to incomplete homogenization between different target lithologies of the crystalline basement and between crystalline basement rock and overlying carbonate rocks.

Acknowledgments–Financial support by the German Science Foundation (DFG) grant KE 732/8–1, –2 is appreciated. Technical assistance for sample preparation and analysis was given by H. Knöfler and P. Czaja. We thank the Chicxulub Scientific Drilling Project of the International Continental Drilling Program and the Universidad Nacional Autónoma de México for providing the Yax-1 drill core samples. The reviews by D. Ames and J. Whitehead improved the quality of the manuscript.

Editorial Handling—Dr. Philippe Claeys

REFERENCES

Allen C. C., Gooding J. L., and Keil K. 1982. Hydrothermally altered impact melt rock and breccia: Contribution to the soil of Mars. *Journal of Geophysical Research* 87:10083–10101.

Alt J. C. 1995. Subseafloor processes in mid-ocean ridge hydrothermal systems. In *Seafloor hydrothermal systems: Physical, chemical, biological and geological interactions,* edited by Humphries S. E., Zierenberg R. A., Mullineaux L. S., and Thomson R. E. Geophysical monograph 91. Washington D.C.: American Geophysical Union. pp. 85–114.

Alvarez L. W., Alvarez W., Asaro F., and Michel H. V. 1980. Extraterrestrial cause for the Cretaceous/Tertiary extinction. *Science* 208:1095–1108.

Ames D. E., Dressler B., Pope K.O., and Pilkington M. 2003. Chicxulub impact structure hydrothermal activity (abstract #07331). *Geophysical Research Abstracts* 5. CD-ROM.

Ames D. E., Watkinson D. H., and Parrish R. R. 1998. Dating of a regional hydrothermal system induced by the 1850 Ma Sudbury impact event. *Geology* 26:447–450.

Berger G., Schott J., and Loubet M. 1987. Fundamental processes controlling the first stage alteration of a basalt by seawater: An experimental study between 200° and 320 °C. *Earth and Planetary Science Letters* 84:431–445.

Bohor B. F. and Glass B. P. 1995. Origin and diagenesis of K/T impact spherules—From Haiti to Wyoming and beyond. *Meteoritics & Planetary Science* 30:182–198.

Claeys P., Heuschkel S., Lounejeva-Baturina E., Sanchez-Rubio G., and Stöffler D. 2003. The suevite of drill hole Yucatán 6 in the Chicxulub impact crater. *Meteoritics & Planetary Science* 38: 1299–1317.

Correns C. W. 1930. Über einen Basalt vom Boden des atlantischen Ozeans und seine Zersetzungsrinde. *Chemie der Erde* 5:76–86.

Dressler B. O. and Reimold W. U. 2001. Terrestrial impact melt rocks and glasses. *Earth-Science Reviews* 56:205–284.

Dressler B. O., Sharpton V. L., and Marin L. E. 2003. Chicxulub Yax-1 impact breccias: Whence they come? (abstract # 1259). 34th Lunar and Planetary Science Conference. CD-ROM.

Dressler B. O., Sharpton V. L., Morgan J., Buffler R., Moran D., Smit J., Stöffler D., and Urrutia J. 2003. Investigating a 65 Ma-old smoking gun: Deep drilling of the Chicxulub impact structure. *EOS Transactions* 84:125–130.

Engelhardt W. V., Luft E., Arndt J., Schock H., and Weiskirchner W. 1987. Origin of modavites. *Geochimica et Cosmochimica Acta* 51:1425–1443.

French B. M., Koeberl C., Gilmour I., Shirey S. B., Dons J. A., and Naterstad J. 1997. The Gardnos impact structure, Norway: Petrology and geochemistry of target rocks and impactites. *Geochimica et Cosmochimica Acta* 61:873–904.

Gonzales-Partida E., Charillo-Chavez A., and Martinez-Ibarra R. 2000. Fluid inclusions from anhydrite related to the Chicxulub crater impact breccias, Yucatán, Mexico: Preliminary report. *International Geology Review* 42:279–288.

Gurov E. P., Koeberl C., and Reimold W. U. 1998. Petrography and geochemistry of target rocks and impactites from the Ilyinets Crater, Ukraine. *Meteoritics & Planetary Science* 33:1317–1333.

Grieve R. A. F. 1978. The melt rocks at Brent crater, Ontario, Canada. Proceedings, 19th Lunar and Planetary Science Conference. pp. 2579–2608.

Grieve R. A. F., Dence M. R., and Robertson P. B. 1977. Cratering processes: As interpreted from the occurrence of impact melts. In *Impact and explosion cratering,* edited by Roddy D. J., Pepin R. O., and Merill R. B. New York: Pergamon Press. pp. 791–814.

Hagerty J. J. and Newsom H. E. 2003. Hydrothermal alteration at the Lonar Lake impact structure, India: Implications for impact cratering on Mars. *Meteoritics & Planetary Science* 38:365–381.

Hecht L., Schmitt R. T., and Wittmann A. 2003. Hydrothermal alteration of the impactites at the ICDP drill site Yax-1 (Chicxulub crater) (abstract # 1979). 34th Lunar and Planetary Science Conference. CD-ROM.

Hildebrand A. R., Penfield G. T., Kring D. A., Pilkington M., Camargo A. Z., Jacobson S. B., and Boynton W. V. 1991. A possible Cretaceous-Tertiary boundary impact crater on the Yucatán Peninsula, Mexico. *Geology* 19:867–871.

Jercinovic M. J., Keil K., Smith M. R., and Schmitt R. A. 1990. Alteration of basaltic glasses from north-central British Columbia, Canada. *Geochimica et Cosmochimica Acta* 54:2679–2696.

Kettrup B., Deutsch A., Ostermann M., and Agrinier P. 2000. Chicxulub impactites: Geochemical clues to the precursor rocks. *Meteoritics & Planetary Science* 35:1229–1238.

Koeberl C. and Sigurdsson H. 1992. Geochemistry of impact glasses from the K/T boundary in Haiti: Relation to smectites and a new type of glass. *Geochimica et Cosmochimica Acta* 56:2113–2129.

Komor S. C., Valley J. W., and Brown P. E. 1988. Fluid inclusion evidence for impact heating at the Siljan Ring, Sweden. *Geology* 16:711–715.

Kring D. A. and Boynton W. V. 1992. Petrogenesis of an augite-bearing melt rock in the Chicxulub structure and its relationship to K/T impact spherules in Haiti. *Nature* 358:141–143.

Le Bas M. J., Le Maitre R. W., Streckeisen A., and Zanettin B. 1986. A chemical classification of volcanic rocks based on the total alkali-silica diagram. *Journal of Petrology* 27:745–750.

Lüders V. and Rickers K. 2004. Fluid inclusion evidence for impact-related hydrothermal fluid and hydrocarbon migration in Creataceous sediments of the ICDP-Chicxulub drill core Yaxcopoil-1. *Meteoritics & Planetary Science.* This issue.

McCarville P. and Crossey L. J. 1996. Post-impact hydrothermal alteration of the Manson impact structure. In *The Manson impact structure, Iowa: Anatomy of an impact crater,* edited by Koeberl C. and Anderson R. R. Special Paper 302. Denver: Geological Society of America. pp. 347–376.

Morgan J., Warner M., Brittan J., Buffler R., Camargo A., Christeson G., Denton P., Hildebrand A., Hobbs R., Macintyre H., Mackenzie G., Maguire P., Marin L., Nakamura Y., Pilkington M., Sharpton V., Snyder D., Suarez G., and Trejo A. 1997. Size and morphology of the Chicxulub impact crater. *Nature* 390:472–476.

Morgan J. V., Warner M. R., Collins G. S., Melosh H. J., and Christeson G. L. 2000. Peak-ring formation in large impact craters: Geophysical constraints from Chicxulub. *Earth and Planetary Science Letters* 183:347–354.

Morgan J. V., Warner M. R., and Grieve R. A. F. 2002. Geophysical constrains on the size and structure of the Chicxulub impact crater. In *Catastrophic events and mass extinctions: Impacts and beyond,* edited by Koeberl C., and MacLeod K. G. Special Paper 356. Boulder: Geological Society of America. pp. 39–46.

Newman A. C. D. 1987. *Chemistry of clays and clay minerals.* Monograph 6. Washington D.C.: Mineralogical Society of America. pp. 480.

Noble D. C. 1967. Sodium, potassium, and ferrous iron contents of some secondarily hydrated natural silicic glasses. *American Mineralogist* 52:280–286.

Osinski G. R., Spray J. G., and Lee P. 2001. Impact-induced hydrothermal activity within the Haughton impact structure, arctic Canada: Generation of a transient, warm, wet oasis. *Meteoritics & Planetary Science* 36:731–745.

Peacock M. A. 1926. The petrology of Iceland, part 1. The basic tuffs. *Transactions of the Royal Society of Edinburgh* 55:53–76.

Pierazzo E. and Melosh H. J. 1999. Hydrocode modeling of Chicxulub as an oblique impact event. *Earth and Planetary Science Letters* 165:163–176.

Reimold W. U., Barr J. M., Grieve R. A. F., and Durrheim R. J. 1990. Geochemistry of the melt and country rocks of the Lake St. Martin impact structure, Manitoba, Canada. *Geochimica et Cosmochimica Acta* 54:2093–2111.

Reimold W. U., Koeberl C., and Bishop J. 1994. Roter Kamm impact crater, Namibia: Geochemistry of basement rocks and breccias. *Geochimica et Cosmochimica Acta* 58:2689–2710.

Schmitt R. T., Wittmann A., and Stöffler D. 2003. The ICDP drill core Yaxcopoil-1, Chicxulub impact crater, Mexico: Shock metamorphism of the impactite units (794–894 m) (abstract # 4061). 34th Lunar and Planetary Science Conference. CD-ROM.

Schmitt R. T., Wittmann A., and Stöffler D. 2004. Geochemistry of drill core samples from Yaxcopoil-1, Chicxulub impact crater, Mexico. *Meteoritics & Planetary Science* 39:979–1001.

Schulte P., Stinnesbeck W., Stüben D., Kramar U., Berner Z., Keller K., and Adatte T. 2003. Fe-rich and K-rich mafic spherules from slumped and channelized Chicxulub ejecta deposits in the northern La Sierrita area, northeast Mexico. *International Journal of Earth Sciences* 92:114–142.

Schuraytz B. C., Sharpton V. L., and Marin L. E. 1994. Petrology of impact-melt rock at the Chicxulub multiring basin, Yucatán, Mexico. *Geology* 22:868–872.

See T. H., Wagstaff J., Yang V, Hörz F., and McKay G. A. 1998. Compositional variation and mixing of impact melts on microscopic scales. *Meteoritics & Planetary Science* 33:937–948.

Sigurdsson H., D'Hondt S., Arthur M. A., Bralower T. J., Zachos J. C., Van Fossen M., and Channell J. E. T. 1991. Glass from the Ctretaceous/Tertiary boundary in Haiti. *Nature* 349:482–487.

Smit J. 1999. The global stratigraphy of the Cretaceous-Tertiary boundary impact ejecta. *Annual Review of Earth and Planetary Sciences* 27:75–113.

Staudigel H. and Hart S. R. 1983. Alteration of basaltic glass: Mechanisms and significance for the oceanic crust-seawater budget. *Geochimica et Cosmochimica Acta* 47:337–350.

Stöffler D., Hecht L., Kenkmann T., Schmitt R. T., and Wittmann A. 2003. Properties, classification, and genetic interpretation of the allochthonous impact formations of the ICDP Chicxulub drill core Yax-1 (abstract # 1553). 34th Lunar and Planetary Science Conference. CD-ROM.

Stöffler D., Artemieva N. A., Ivanov B. A., Hecht L., Kenkmann T., Schmitt R. T., Tagle R. A., and Wittmann A. 2004. Origin and emplacement of the impact formations at Chicxulub, Mexico, as revealed by the ICDP deep drilling at Yaxcopoil-1 and by numerical modeling. *Meteoritics & Planetary Science.* This issue.

Stroncik N. A. and Schmincke H. U. 2002. Palagonite—A review. *International Journal of Earth Sciences* 91:680–697.

Sturkell E. F. F., Broman C., Forsberg P., and Torssander P. 1998. Impact-related hydrothermal activity in the Lockne impact structure, Jamtland, Sweden. *European Journal of Mineralogy* 10:589–606.

Utzmann A., Hansteen T. H., and Schmincke H. U. 2002. Trace element mobility during sub-seafloor alteration of basaltic glass from Ocean Drilling Program site 953 (off Gran Canaria). *International Journal of Earth Sciences* 91:661–679.

Wedepohl K. H. 1995. The composition of the continental crust. *Geochimica et Cosmochimica Acta* 59:1217–1232.

Wittmann A., Kenkmann T., Schmitt R. T., and Stöffler D. 2003. Clastic polymict dikes in the "megablock" sequence of the ICDP-Chicxulub drill core Yax-1 (abstract # 1386). 34th Lunar and Planetary Science Conference. CD-ROM.

Wittmann A., Kenkmann T., Schmitt R. T., Hecht L., and Stöffler D. 2004. Impact-related dike breccia lithologies in the ICDP drill core Yaxcopoil-1, Chicxulub impact structure, Mexico. *Meteoritics & Planetary Science* 39:931–954.

Zhou Z. and Fyfe W. S. 1989. Palagonitization of basaltic glass from DSDP site-335, LEG-37—Textures, chemical composition, and mechanism of formation. *American Mineralogist* 74:1045–1053.

Zürcher L. and Kring D. A. 2003. Preliminary results on the post-impact hydrothermal alteration in the Yaxcopoil-1 hole, Chicxulub impact structure, Mexico (abstract # 1735). 34th Lunar and Planetary Science Conference. CD-ROM.